DMD Fast Forward. Published on January 7, 2008 as doi:10.1124/dmd.107.019596
This article has not been copyedited and formatted. The final version may differ from this version.

GLUCURONIDATION OF POLYCHLORINATED BIPHENYLOLS AND UDPGA CONCENTRATIONS IN CHANNEL CATFISH LIVER AND INTESTINE

James C. Sacco, Hans-Joachim Lehmler, Larry W. Robertson, Wenjun Li and Margaret O. James

Department of Medicinal Chemistry, College of Pharmacy, University of Florida, PO Box 100485, Gainesville, FL 32610, USA (JCS, MOJ, WL) and Department of Occupational and Environmental Health, College of Public Health, University of Iowa, Iowa City, IA, USA (HJL, LWR)

Running title: Glucuronidation of hydroxy-PCBs in catfish tissues

Corresponding author:

Margaret O. James

Department of Medicinal Chemistry

University of Florida

PO Box 100485

Gainesville

FL 32610-0485

USA

Telephone: 1 352 273 7707

Fax: 1 352 846 1972

Email: mojames@ufl.edu

Number of text pages: 32

Number of tables: 4

Number of figures: 7

Number of references: 38

Number of words in the Abstract: 250

Number of words in the Introduction: 749

Number of words in the Discussion: 1513

List of non-standard abbreviations: OH-PCB, polychlorinated biphenylol; PCB, polychlorinated biphenyl; PIC-A, tetrabutylammonium sulfate; UDPGA, uridine-5'-diphospho-glucuronic acid; UGT, uridine-diphospho-glucuronosyltransferase.

Abstract

Polychlorinated biphenylols (OH-PCBs) are potentially toxic PCB metabolites that can be eliminated by glucuronidation, catalyzed by UDP-glucuronosyltransferases (UGTs). OH-PCBs with a 3,5-dichloro-4-hydroxy- substitution pattern have been detected in blood from humans and wildlife, suggesting slow elimination. This study assessed the glucuronidation of 4-OH-PCBs with 0, 1 or 2 Cl atoms flanking the 4-hydroxyl group, and 0 to 4 Cl atoms in the aphenolic ring, in microsomes from channel catfish liver and proximal intestine. Product formation was quantitated with ^{14}C- UDP-glucuronic acid (UDPGA). Physiologic concentrations of UDPGA were measured in preparations of liver and intestine. When varying the OH-PCB concentrations in the presence of saturating UDPGA concentrations, glucuronidation V_{max} values were higher in hepatic than intestinal microsomes (0.40-3.4 and 0.12-0.78 nmole/min/mg protein, respectively), while the K_m values were generally lower for intestine (0.042-0.47 mM) than liver (0.11-1.64 mM). In both tissues V_{max} values with 3,5-dichloro-4-OH-PCBs were lower than with the corresponding 3-chloro-4-OH-PCBs. Varying the UDPGA concentrations in the presence of saturating concentrations of OH-PCB showed the K_m for UDPGA was lower in intestine (27 µM) than liver (690 µM). The measured concentration of UDPGA in catfish liver (246 to 377 nmole/g) was lower than the K_m for UDPGA, suggesting *in vivo* rates of glucuronidation may be sub-optimal, while in intestine the measured UDPGA concentration (71 to 258 nmole/g) was higher than the K_m for UDPGA. Although liver has greater glucuronidation capacity than proximal intestine, the properties of intestinal UGTs in channel catfish enable them to efficiently glucuronidate low concentrations of OH-PCBs.

Introduction

Polychlorinated biphenyls (PCBs) are ubiquitous environmental contaminants, found at all trophic levels around the globe (Erickson, 2001). Biotransformation is an important influence on PCB toxicokinetics in animals, and depends on congener structure and the animal's metabolic capacity. Polychlorinated biphenylols (OH-PCBs) are products of cytochrome P450-dependent hydroxylation of PCBs (James, 2001). While OH-PCBs are more water-soluble than their parent molecules, they are still lipophilic enough to be orally absorbed, and distribute to tissues (Sinjari and Darnerud, 1998). Several OH-PCBs have been detected in the plasma and tissues of animals, including catfish (Li et al., 2003), and humans (Sandau et al., 2002). Plasma OH-PCBs probably arise from recent dietary exposure, biotransformation of PCBs, and perhaps enterohepatic cycling of OH-PCB conjugates. Laboratory studies demonstrated that rats given PCBs excreted OH-PCBs in milk, as evidenced by the presence of OH-PCBs in the stomach contents of nursing pups (Fielden et al., 2001). OH-PCBs may contribute to the recognized toxic effects of PCBs such as endocrine disruption, tumor promotion and neurological dysfunction (Machala et al., 2004; Meerts et al., 2004; Arulmozhiraja et al., 2005).

The expected pathways of elimination of these toxic metabolites are glucuronidation and sulfonation, yet few studies have examined the conjugation of OH-PCBs (Tampal et al., 2002; Daidoji et al., 2005; Sacco and James, 2005; Wang et al., 2006) particularly by glucuronidation, which is normally a higher-capacity pathway than sulfonation. Glucuronidation is catalyzed by a family of microsomal enzymes, the UDP-glucuronosyltransferases (UGTs), and requires the co-substrate uridine 5`-diphosphoglucuronic acid (UDPGA). UGTs are expressed in the liver and extrahepatic tissues (Daidoji et al., 2005).

The various chlorine and hydroxyl substitution patterns possible on the biphenyl structure may lead to significant differences in glucuronidation kinetics. One possible explanation for the slow elimination of certain OH-PCBs is that they are poor substrates for glucuronidation. The efficiency of glucuronidation of several mostly *para*-OH-PCBs by rat liver microsomes varied widely, and substitution of chlorine atoms at the *meta*- and *para*-positions on the aphenolic ring lowered V_{max} (Tampal et al., 2002). In rats, liver microsomes exhibited higher V_{max} values and enzyme efficiencies for glucuronidation of OH-PCBs than the large and small intestine, lung, kidney or testis (Daidoji et al., 2005). An exception was that compared with the liver, the rat intestine had similar or higher efficiencies of glucuronidation for two of the substrates studied, 4'-OH-CB121 and 4'-OH-CB159.

Most of the persistent OH-PCBs found in human plasma are hydroxylated at the *para*-position and *meta*-chlorinated on either side of the phenolic group. The remaining substitution pattern on both rings is highly variable (Bergman et al., 1994). A hydroxyl group in the *para* position with two flanking chlorine atoms is associated with inhibition of sulfotransferases (Kester et al., 2000; Wang et al., 2005) and high affinity for the major transport protein for thyroid hormone, transthyretin (Lans et al., 1993).

The other variable that can influence the rate of glucuronidation of a xenobiotic is the tissue concentration of UDPGA. When conducting *in vitro* studies, it is common practice to employ saturating concentrations of UDPGA, so that maximal UGT activity will be observed. Thus, millimolar concentrations of UDPGA are usually used to determine the aglycone kinetic parameters for glucuronidation reactions. Measured hepatic UDPGA concentrations in mammals were in the range of 120-500 μM (Zhivkov et al., 1975; Cappiello et al., 1991; Goon and Klaassen, 1992), and in fish were 21 μM (carp) and 115 μM (trout) (Zhivkov et al., 1975).

The rate of glucuronidation of 3-OH-benzo(a)pyrene in guinea pig intestinal epithelial cells was found to be dependent on the endogenous level of UDPGA (Singh et al., 1986), as was glucuronidation of 7-hydroxycoumarin in rat liver (Conway et al., 1988). The efficacy of glucuronidation of a xenobiotic could be overestimated because the maximal rate determined by conventional kinetic experiments may be greater than the maximal rate that is possible *in vivo*.

Fish are a recognized dietary source of PCBs and other persistent organic pollutants (Sjödin et al., 2000). Hydroxylation of PCBs occurs in fish, though more slowly than in rats or humans (James, 2001). In an isolated perfused intestinal preparation from the channel catfish, 3,3',4,4'-tetrachlorobiphenyl (CB-77) was only slowly metabolized (Doi et al., 2006). Unconjugated OH-PCBs were identified in intestinal mucosa and blood, suggesting slow conjugation in fish intestine, which may impair the elimination of OH-PCBs.

The objectives of the present study were to investigate the capability of microsomes from channel catfish liver and proximal intestine to glucuronidate a series of *para*-OH-PCBs and to assess physiologic concentrations of UDPGA in liver and proximal intestine.

Materials and Methods

Chemicals. A total of 18 substrates were used in this study (Figure 1). The nomenclature of the OH-PCBs as PCB metabolites is based on the recommendations of Maervoet and co-workers (Maervoet et al., 2004). The following substrates (Catalog no. in parentheses) were purchased from Accustandard (New Haven, CT): 4-OH-CB1 (1002N), 4-OH-CB2 (1003N), 4′-OH-CB9 (2003N), 4-OH-CB14 (2004N), 4′-OH-CB18 (3004N), 4'-OH-CB69 (4008N), 4'-OH-CB72 (4009N), 4'-OH-CB106 (5005N), 4'-OH-CB112 (5006N), 4'-OH-CB121 (5007N), 4'-OH-CB159 (6001N), and 4'-OH-CB165 (6002N). The compounds 4′-OH-CB3, 4'-OH-CB35, 4-OH-CB39, 4'-OH-CB68, 4'-OH-CB79 were synthesized by Suzuki-coupling as described previously (Lehmler and Robertson, 2001). The 4-hydroxy biphenyl (4-OH-BP) was purchased from Sigma (St.Louis, MO). ^{14}C-UDPGA (196 μCi/μmol) was obtained from PerkinElmer Life and Analytical Sciences (Boston, MA). The ^{14}C-UDPGA was diluted with unlabelled UDPGA to a specific activity of 1.5-5 μCi/μmol for use in enzyme assays. PIC-A (tetrabutylammonium hydrogen sulfate) was obtained from Waters Corp. (Milford, MA). Other reagents were the highest grade available from Fisher Scientific (Atlanta, GA) and Sigma.

Animals. Adult channel catfish (*Ictalurus punctatus*) aged approximately 2.5 years, body weight 2.1 – 3.7 kg, were used for study of OH-PCB glucuronidation. Adult catfish aged approximately 1.5 years, body weight 0.75 – 1.7 kg were used for measurement of UDPGA concentrations. All fish were kept in flowing well water and fed a fish chow diet (Silvercup, Murray, UT). Care and treatment of the animals was conducted as per the guidelines of the University of Florida Institutional Animal Care and Use Committee. The microsomal fractions were obtained from liver and proximal intestinal mucosa using a procedure described previously (James et al., 1997), and stored in aliquots at -80°C. Samples of liver and whole intestinal mucosa for determination

of UDPGA concentrations were taken from catfish sacrificed in November and were snap frozen and stored at -80°C until analysis. Protein determination was carried out by the Lowry method using bovine serum albumin as protein standard.

Glucuronidation assay. A radiochemical ion-pair extraction method was employed to investigate the glucuronidation of the 4-OH-PCBs and 4-OH-BP (Wang et al., 2004). Substrate consumption did not exceed 10%. Initial experiments determined the saturating concentrations of UDPGA to be employed, and linearity with protein and time. Duplicate tubes were used for each measurement. The incubation mixture consisted of 0.1 M Tris-Cl buffer (*p*H 7.6), 5mM $MgCl_2$, 50 µg Brij-58, 100 µg catfish intestinal or hepatic microsomal protein, varying concentrations of ^{14}C-UDPGA, and varying concentrations of OH-PCB substrate in a total reaction volume of 0.1 mL. Blanks contained all components except the OH-PCB. The OH-PCBs were added to tubes from methanol solutions and the solvent removed under nitrogen. Mixtures of microsomal protein and Brij-58 were added to the dried substrate, vortex-mixed and left on ice for 30 minutes. Subsequently, the buffer, $MgCl_2$, and water were added. After a pre-incubation of 3 minutes at 35ºC, the optimum temperature for catfish UGT activity, ^{14}C-UDPGA was added to initiate the reaction, which was terminated after 30 minutes incubation by the addition of a 1:1 mixture of 2.5% acetic acid and PIC-A, 0.1 mL, and water, 0.3 mL. The ion-pair of the glucuronide product was extracted into ethyl acetate, 2 x 1.5 mL. For each tube, duplicate portions of the combined ethyl acetate phases were counted for quantitation of glucuronide conjugate and results were averaged.

The extraction assay was validated with three substrates, 4'OH-CB69, 4'OH-CB112 and 4'OH-CB121. For each of these substrates, and for incubation of microsomes with ^{14}C-UDPGA but no substrate, portions of the ethyl acetate extracts were evaporated to dryness and taken up in

0.1 mL ethanol. For incubations with the OH-PCBs additional residues from the dried ethyl acetate extracts were taken up in 0.1 mL Tris-Cl buffer, pH 6 or 0.1 mL Tris-Cl buffer pH 6 containing 7,500 units of β-glucuronidase. The tubes with Tris buffer were incubated at 37°C for 16 hr, then 0.1 mL ethanol was added. Samples of each (0.04 mL) as well as samples of the aqueous phase from the incubations (0.005 mL) were applied to the pre-adsorbent phase of LK5DF plates (Whatman, Florham Park, NY). Plates were developed in a solvent system containing 1-butanol: acetone: acetic acid: ammonium hydroxide: water, 50:25:9:0.75:15 by volume. Dried plates were placed in a Packard Instant Imager to visualize and quantitate the radioactivity by electronic autoradiography.

Measurement of UDPGA. Liver tissue or intestinal mucosa, 0.1g, was mechanically homogenized with 0.4 mL of 0.3 M mono-basic ammonium phosphate. The tube containing the homogenate was placed in a boiling water bath for 1 minute then removed, cooled and the contents re-homogenized. The tube was centrifuged at 600 g for 20 min, and the cloudy supernatant was transferred into a 1.5 mL microcentrifuge tube and centrifuged for 15 minutes at 16,000 g. The supernatant was then filtered by centrifugation in 0.45 μM Spin-filters (Costar, Corning Inc., NY). An aliquot, 50 μL, of this sample was analyzed by anion exchange HPLC (Model 2300 pump, ISCO, Lincoln, NE, with a Dynamax UV absorbance detector, Rainin, Woburn, MA). HPLC conditions were an isocratic mobile phase of 0.14 M ammonium phosphate buffer, pH 3.0) at 1 mL/min and a Zorbax SAX column stationary phase (Agilent, Palo Alto, CA, column size 4.6 mm i.d. x 250 mm, 5 μM), with UV detection at 260 nm.

Physicochemical parameters. For each OH-PCB and 4-OH-BP, the pK_a of the phenolic group was calculated using SPARC software (Hilal et al., 1995). Other structural properties, such as

log P, dihedral angle and molecular size were calculated with software, ACD/ILab (Advanced Chemistry Development, Ontario, Canada) or ChemDraw 3D (CambridgeSoft, Cambridge, MA).

Data analysis. Duplicate values for the rate of conjugate formation at each substrate concentration were used to calculate kinetic parameters using Prism v4.0 (GraphPad Software, Inc., San Diego, CA). Equations used to fit the data were the Michaelis-Menten equation for one-site binding and the Hill plot for positive cooperativity. The best fit to each equation was selected as the results for each data set. Relationships between structural features and kinetic parameters were analyzed by linear or non-linear regression and statistical differences examined by ANOVA with post-hoc tests using Prism 4.0.

Results

Validation of assay method. The tetrabutylammonium ion-pairs of the glucuronide conjugates of 4′-OH-CB69, 4′-OH-CB112 and 4′-OH-CB121 were shown by TLC analysis and autoradiography to be completely extracted into ethyl acetate, with no conjugate detected in the aqueous phase. Results for 4′-OH-CB121 are shown in figure 2. The glucuronide conjugate of 4′-OH-CB121 had an R_F of 0.74, glucuronic acid released by hydrolysis an R_F of 0.28 and unreacted UDPGA did not move from the origin. TLC analysis of the ethyl acetate extracts (Figure 2, lanes 1 and 2) showed that no ^{14}C-UDPGA was extracted into ethyl acetate, and that incubation of microsomes alone with ^{14}C-UDPGA did not reveal detectable conjugates. TLC analysis of the aqueous phases (Figure 2, lanes 5 and 6) showed that no glucuronide conjugate remained in the aqueous phase. Figure 2 (lanes 3 and 4) also shows that the glucuronide of 4′-OH-CB121 was hydrolyzed by β-glucuronidase but not by incubation in buffer alone. Similar results were obtained with the other substrates tested.

With all substrates, assay duplicates showed less than 2% difference from the mean. Although no conjugate can be observed in lane 2 of Figure 2, a small amount of radioactivity was extracted from incubations that contained microsomes but no substrate, and rates of glucuronidation were corrected for this background. Incubations with no substrate and no microsomes showed no detectable counts in the ethyl acetate extracts.

Kinetics of UDPGA. The kinetic parameters when varying the concentration of UDPGA were determined for the glucuronidation of three OH-PCBs (Table 1). The apparent K_m values for UDPGA were more than 10-fold higher in the liver than in the intestine. The concentrations of UDPGA used for studies of OH-PCB substrate kinetics were such that maximal rates were

measured, and were 1.5 mM for liver microsomes and 0.2 mM for proximal intestinal microsomes.

Aglycone kinetics. The glucuronidation of most of the OH-PCBs tested followed Michaelis-Menten kinetics in hepatic and intestinal microsomes. Figure 3A shows representative results with hepatic microsomes from 4 individual catfish for 4'-OH-CB159. In the case of the glucuronidation of 4′-OH-CB18 and 4'-OH-CB112 by proximal intestine and 4'-OH-CB35 by liver, the data showed positive cooperativity and fitted the Hill plot. Results for glucuronidation of 4'-OH-CB112 by proximal intestinal microsomes are shown in Figure 3B. The estimated apparent maximal rate of glucuronidation of polychlorinated biphenylols by channel catfish ranged from 124-784 pmol/min/mg for proximal intestine and 317-2,838 pmol/min/mg for the liver (Table 2). Compared to the other substrates tested, 4'-OH-CB18 and 4'OH-CB69 were very efficiently glucuronidated by the intestine; these substrates were less efficiently glucuronidated by liver microsomes. The efficiencies of glucuronidation of 4′-OH-CB3, 4′-OH-CB9, 4'-OH-CB79, 4'-OH-CB106 and 4'-OH-CB112 were similar in intestinal and hepatic microsomes, while the other OH-PCBs studied exhibited higher rates of clearance in liver than in intestine (Table 2). As has been found previously in studies of fish, there was considerable inter-individual variability in the kinetic parameters.

The uncorrected microsomal protein yield was 4.7 ± 0.5 mg/g (mean ± SEM, n=9) in proximal intestine and 12.4 ± 1.5 mg/g in liver (n=4). The total microsomal protein per organ was significantly higher in liver (442 ± 54 mg in whole liver) than proximal intestine (32 ± 6 mg in intestinal mucosa). Because there is an order of magnitude more microsomal protein in the total liver than in the proximal intestinal mucosa, then under optimal *in vitro* assay conditions the

DMD Fast Forward. Published on January 7, 2008 as DOI: 10.1124/dmd.107.019596
This article has not been copyedited and formatted. The final version may differ from this version.

liver should be quantitatively the major organ of glucuronidation of all the studied OH-PCB in the channel catfish.

With the exceptions of 4-OH-CB1, 4-OH-CB2 and 4'-OH-CB165, K_m values for individual OH-PCBs were different in the liver than in the intestine. For most of the OH-PCBs studied, the K_m values for intestinal catfish UGTs (K_m range: 15-572 μM) were lower than for liver UGTs (K_m range: 57-1,643 μM). V_{max} values were significantly higher in liver than in intestine ($p<0.01$). The V_{max} values of OH-PCB glucuronidation in liver and intestine were correlated with each other ($r^2=0.36$), as shown in Figure 4. This relationship did not exist for K_m values.

Structural influences and physico-chemical properties. Five structurally related OH-PCB pairs were studied, in which the chlorine substitution pattern in the aphenolic ring was constant, while the phenolic ring had one or two Cl atoms flanking the hydroxyl group. The V_{max} values for glucuronidation in both proximal intestine and liver were significantly decreased upon addition of a second chlorine substituent flanking the phenolic moiety, $p<0.01$ (Figure 5).

The effect of position and number of chlorine substituents in the aphenolic ring on the glucuronidation of OH-PCBs was also investigated. No significant differences in K_m and V_{max} values were observed with the absence or presence of specific chlorine substituents on the aphenolic ring. Weak negative correlations were found between K_m values in intestine and parameters related to molecular size and lipophilicity. Similar weak negative correlations were found between V_{max} values in liver and the same parameters (data not shown).

The kinetic parameters of the OH-PCBs studied were grouped according to whether there were 0, 1 or 2 Cl atoms flanking the OH group, and the mean values for K_m and V_{max} compared for liver and intestine. This analysis showed that in liver, both V_{max} and K_m values were higher

for OH-PCBs with one Cl atom flanking the OH group than those with 0 or 2 flanking Cl atoms (Table 3). In intestine, OH-PCBs with two Cl atoms flanking the OH group showed lower V_{max}, than those with zero or one. It is known that Cl atoms adjacent to the phenolic OH group affect the pK_a of chlorophenols and chlorobiphenylols. Plots of pK_a versus V_{max} for each OH-PCB and including the non-chlorinated 4-OH-BP revealed a trend for higher V_{max} values with compounds that have pK_a values between 7 and 8 in liver and between 7 and 8.5 in intestine (Figure 6).

UDPGA concentration in liver and intestine. The HPLC method developed for measuring UDPGA concentrations was effective in resolving this analyte from other UV_{260} absorbing compounds in extracts of liver and intestinal mucosa. Replicates from different regions of the liver were less than 5% different from each other. The mean UDPGA concentration in the catfish liver, 325 ± 19 nmol/g (mean ± SEM, n=7) was higher than in the intestine, 136 ± 35, n = 5, $p<0.01$. As seen in figure 7, there was considerable inter-individual variability in UDPGA concentrations from the intestine of the catfish studied.

Discussion

For OH-PCBs, as for other xenobiotics with one phenolic group and no other polar substituents (Wang et al., 2004), adding PIC-A in the assay stop solution, then extracting the conjugate ion pair into ethyl acetate, is a rapid, sensitive method for measuring rates of glucuronidation of suitable substrates.

Microsomal glucuronidation V_{max} values of the 4-OH-PCBs studied and 4-OH-BP were lower in proximal intestine than in liver, and for most compounds, K_m values were also lower in intestine than liver, suggesting that intestinal UGTs have higher affinity for OH-PCB substrates than liver. The total capacity of the liver for glucuronidation of OH-PCBs is much greater than that of the intestine when the total content of microsomal protein in these two organs is considered. The yield of microsomal protein from liver was twice that of the intestine, possibly because of the decreased amount of endoplasmic reticulum in enterocytes relative to hepatocytes (DePierre et al., 1987). The greater size of the liver meant the total amount of microsomal protein in liver was more than ten times that in the proximal intestine. Thus, the overall capacity of the liver under optimal conditions for glucuronidation is considerably higher than the intestine. However, biotransformation in the intestine is important for orally ingested xenobiotics, and the greater efficiency of the intestinal UGTs at low concentrations of OH-PCBs suggests it plays an important role in protecting the organism from these potentially toxic compounds.

These results suggest that liver and proximal intestine have different UGT isoform profiles, with the intestine possessing one or more isoforms that display greater efficiency than the liver for OH-PCBs. We have cloned several UGT isoforms from catfish liver and intestine whose characteristics support this view (Sacco, 2006). UGT isoforms responsible for efficient

OH-PCB glucuronidation may be catfish enzymes analogous to rat UGT1A1, UGT1A6 and UGT2B1 (Daidoji et al., 2005).

Of the substrates studied, 4′-OH-CB18 was glucuronidated most readily in the channel catfish intestine and liver, with efficiencies of 47 and 20.8 µL/min/mg protein, respectively. The poorest substrates were 4-OH-CB14 in the intestine, with an efficiency of 0.7 µL/min/mg protein and 4′-OH-CB3, 4′-OH-CB9 and 4′-OH-CB112 in the liver all with efficiencies of 1.4 µL/min/mg protein. Nine of the compounds studied in catfish were studied in rat liver (Tampal et al., 2002; Daidoji et al., 2005), namely 4′-OH-CB3, 4-OH-CB14, 4-OH-CB39, 4′-OH-CB35, 4′-OH-CB68, 4′-OH-CB69, 4′-OH-CB79, 4′-OH-CB121 and 4′-OH-CB159. There was no correlation in V_{max}, K_m, or enzyme efficiency for these compounds between catfish liver and rat liver or between catfish intestine and rat liver ($p>0.05$). All these compounds were glucuronidated most efficiently in rat liver microsomes, with a mean 24-fold higher efficiency than catfish liver (range of 5 to 55-fold higher in rat) and 47-fold higher efficiency than catfish intestine (range of 7- to 173-fold higher in rat liver). While the greater efficiencies of glucuronidation in rat than catfish may be ascribed to differences in UGT isoform type, properties and level of expression, this is an important difference, since glucuronidation is likely to be the major pathway for elimination of OH-PCBs. The relatively poor glucuronidation efficiencies in catfish liver and intestine suggest that both bioavailability and elimination half-lives of OH-PCBs will be higher than in rat, leading to greater exposure of catfish to potentially toxic OH-PCBs.

Since microsomes contain a heterogeneous population of UGTs exhibiting different levels of expression and activity, it was not the major objective of this study to attempt to predict the effect of molecular structure and physicochemical parameters on the glucuronidation of OH-

PCBs, which is better achieved using individual isoforms. However, effects observed at a microsomal level are likely to reflect processes that occur in the intact organism, where multiple UGTs contribute to substrate glucuronidation. Recognizing structural features that affect K_m and V_{max} may help to further delineate the different toxicokinetics of OH-PCBs.

OH-PCBs with two chlorine atoms flanking the OH group exhibited lower V_{max} values than compounds with one flanking chlorine, in catfish liver and proximal intestine (Figure 5). For example, while 4′-OH-CB35 was a good substrate for glucuronidation, addition of a second chlorine flanking the –OH group as in 4′-OH-CB79 resulted in a greater decrease in V_{max} than the addition of two adjacent chlorine substituents on the aphenolic ring as in 4′-OH-CB106. The effect of a second flanking chlorine atom on V_{max} is interesting from a toxicological standpoint since almost all the OH-PCBs identified in human plasma feature a 4-hydroxy-3,5-dichloro- pattern (Fängström et al., 2002; Hovander et al., 2002; Sandau et al., 2002). It is possible that one reason for the persistence of these OH-PCBs may be slow glucuronidation due to this structural arrangement.

Further examination of the effect of chlorine substitution adjacent to the 4-hydroxyl group revealed the pattern that V_{max} was highest in liver for compounds with one adjacent chlorine atom, compared with zero or two, while in intestine, compounds with two chlorines flanking the hydroxyl group had the lowest V_{max} values (Table 3). The physicochemical property most strongly influenced by the presence of adjacent chlorine atoms is the acidity of the phenolic group. The estimated pK_as for OH-PCBs with two flanking chlorine substituents were significantly lower than for similar molecules with one flanking chlorine, and those with one flanking chlorine had lower pK_a values than those with no flanking chlorines (Hilal et al., 1995; Tampal et al., 2002). In catfish, V_{max} values for glucuronidation were highest if the estimated pK_a

of the OH-PCB was in the range 7-8 for liver microsomes and 7-8.5 for proximal intestinal microsomes (Figure 6). At physiological pH, and the assay pH, substrates with *pKa* values in this range will have approximately half the molecules of OH-PCB in the ionized form, while those with lower or higher pKa values will have greater or fewer proportionately as the anion. Ease of protonation/deprotonation is likely to influence the interaction of the hydroxyl group with a critical histidine residue in the aglycone binding site that is thought to form part of a charge-relay system important in transfer of the glucuronide (Radominska-Pandya et al., 2005; Locuson and Tracy, 2007). Lipophilicity and molecular size may also influence kinetic properties, but in this study, only weak associations with these parameters were observed.

Catfish liver UDPGA concentrations were similar to those previously reported for mammals, such as humans (279 μM), rats (400 μM), and guinea pigs (413 μM) (Cappiello et al., 1991; Goon and Klaassen, 1992; Yamamura et al., 2000) and higher than we found from catfish sacrificed in the month of May (133 μM) (James et al., 2007). The results reported for trout (116 μM) and carp (21 μM) liver (Zhivkov et al., 1975) are lower than the levels measured in this study (Figure 6). Intestinal UDPGA concentrations in the catfish were in the range reported for rat intestine (121 ± 5 μM) (Goon and Klaassen, 1992), but higher than humans (19 ± 5 μM) (Cappiello et al., 1991) and lower than guinea pigs (322 ± 5 μM) (Zhivkov et al., 1975). These differences may be species-related, or influenced by nutritional or physiological changes influenced by season. Another possible contributor to the discrepancy is that different analytical techniques were used. The values for trout and carp (Zhivkov et al., 1975) were determined from liver homogenized in perchloric acid in order to solubilize the nucleotides. This may have led to hydrolysis of UDPGA to UDP and glucuronic acid, which has been shown to increase with decreased pH (Bedford et al., 2003).

Hepatic UDPGA concentrations in channel catfish taken in the month of November (this study) were in the range of 246-371 μM. The UDPGA K_m values obtained for hepatic glucuronidation were 684 μM and 697 μM for 4′-OH-CB72 and 4′-OH-CB35, respectively (Table 1). This means that, *in vivo*, hepatic glucuronidation would proceed at a suboptimal rate both for 4′-OH-CB72 and 4′-OH-CB35. In the intestine, UDPGA concentrations ranged from 71-255 μM, higher than the UDPGA K_m of 27 μM found for 4′-OH-CB69 in proximal intestinal microsomes (Table 1). The UGT isoforms in the intestine responsible for OH-PCB glucuronidation appear to work optimally at much lower concentrations of UDPGA than in liver, and thus are well-equipped to catalyze the conjugation of low concentrations of OH-PCBs.

In summary the different K_m values estimated for glucuronidation of a series of 4-OH-, 4-OH-3-chloro- and 4-OH-3,5-dichloro-PCBs suggest differences in the UGT isozyme profile of catfish liver and proximal intestine. The rates of maximal glucuronidation for all substrates tested were higher for the liver than the intestine, and were optimal for substrates whose pK_a values favored transfer of the phenolic proton. The V_{max} values for both hepatic and intestinal glucuronidation were lower in compounds with two chlorine atoms flanking the phenolic group, an arrangement typical of OH-PCBs that persist in organisms. The K_m for UDPGA in catfish liver was more than double the measured hepatic concentration of UDPGA, suggesting that glucuronidation in the intact liver will proceed more slowly than was measured *in vitro* in the presence of excess UDPGA. In the intestine, however, the measured concentrations of UDPGA were four times higher than the UDPGA K_m value, suggesting that enzyme efficiencies measured *in vitro* will approximate the expected *in vivo* rate of glucuronidation of OH-PCBs.

Acknowledgements

The authors thank Laura Rowland Faux and Ran Zheng for their assistance.

References:

Arulmozhiraja S, Shiraishi F, Okumura T, Iida M, Takigami H, Edmonds JS and Morita M (2005) Structural requirements for the interaction of 91 hydroxylated polychlorinated biphenyls with estrogen and thyroid hormone receptors. *Toxicol Sci* **84:**49-62.

Bedford CT, Hickman AD and Logan CJ (2003) Structure-activity studies of glucose transfer: determination of the spontaneous rates of hydrolysis of uridine 5'-diphospho-alpha-D-glucose (UDPG) and uridine 5'-diphospho-alpha-D-glucuronic acid (UDPGA). *Bioorg Med Chem* **11:**2339-2345.

Bergman Å, Klasson-Wehler E and Kuroki H (1994) Selective retention of hydroxylated PCB metabolites in blood. *Environ Health Perspect* **102:**464-469.

Cappiello M, Giuliani L and Pacifici GM (1991) Distribution of UDP-glucuronosyltransferase and its endogenous substrate uridine 5'-diphosphoglucuronic acid in human tissues. *Eur J Clin Pharmacol* **41:**345-350.

Conway JG, Kauffman FC, Tsukuda T and Thurman RG (1988) Glucuronidation of 7-hydroxycoumarin in periportal and pericentral regions of the lobule in livers from untreated and 3-methylcholanthrene-treated rats. *Mol Pharmacol* **33:**111-119.

Daidoji T, Gozu K, Iwano H, Inoue H and Yokota H (2005) UDP-glucuronosyltransferase isoforms catalyzing glucuronidation of hydroxy-polychlorinated biphenyls in rat. *Drug Metab Dispos* **33:**1466-1476.

DePierre JW, Andersson G and Dallner G (1987), in: *The Liver: Biology and Pathobiology* (Arias IM, Jakoby WB, Popper H, Schachter D and Shafritz DA eds), pp 165-187, Raven Press, New York.

Doi AM, Lou Z, Holmes E, Venugopal CS, Nyagode B, James MO and Kleinow KM (2006) Intestinal bioavailability and biotransformation of 3,3',4,4'-tetrachlorobiphenyl (CB 77) in in situ preparations of channel catfish following dietary induction of CYP1A. *Aquat Toxicol* **77:**33-42.

Erickson MD (2001) Introduction: PCB properties, uses, occurrence and regulatory history. , in: *PCBs. Recent Advances in the Environmental Toxicology and Health Effects* (Robertson LW and Hansen LG eds), pp 35-45, The University Press of Kentucky, , Lexington, KY.

Fängström B, Athanasiadou M, Grandjean P, Weihe P and Bergman Å (2002) Hydroxylated PCB metabolites and PCBs in serum from pregnant Faroese women. *Environ Health Perspect* **110:**895-899.

Fielden MR, Halgren RG, Tashiro CH, Yeo BR, Chittim B, Chou K and Zacharewski TR (2001) Effects of gestational and lactational exposure to Aroclor 1242 on sperm quality and in vitro fertility in early adult and middle-aged mice. *Reprod Toxicol* **15:**281-292.

Goon D and Klaassen CD (1992) Effects of microsomal enzyme inducers upon UDP-glucuronic acid concentration and UDP-glucuronosyltransferase activity in the rat intestine and liver. *Toxicol Appl Pharmacol* **115:**253-260.

Hilal SH, Karickhoff SW and Carreira LA (1995) A Rigorous Test for SPARC's Chemical Reactivity Models: Estimation of More Than 4300 Ionization pKa's. *Quantitative Structure-Activity Relationships* **14:**348-355.

Hovander L, Malmberg T, Athanasiadou M, Athanassiadis I, Rahm S, Bergman Å and Wehler EK (2002) Identification of hydroxylated PCB metabolites and other phenolic halogenated pollutants in human blood plasma. *Arch Environ Contam Toxicol* **42:**105-117.

James MO (2001) Polychlorinated biphenyls: metabolism and metabolites., in: *PCBs- Recent Advances in Environmental Toxicology and Health Effects* (Robertson LW and Hansen LG eds), pp 35-46, University of Kentucky Press, Lexington.

James MO, Altman AH, Morris K, Kleinow KM and Tong Z (1997) Dietary modulation of phase 1 and phase 2 activities with benzo(a)pyrene and related compounds in the intestine but not the liver of the channel catfish, Ictalurus punctatus. *Drug Metab Dispos* **25:**346-354.

James MO, Sacco JC and Faux LR (2007) Effects of food natural products on the biotransformation of PCBs. *Environmental Toxicology and Pharmacology* **in press**.

Kester MH, Bulduk S, Tibboel D, Meinl W, Glatt H, Falany CN, Coughtrie MW, Bergman Å, Safe SH, Kuiper GG, Schuur AG, Brouwer A and Visser TJ (2000) Potent inhibition of estrogen sulfotransferase by hydroxylated PCB metabolites: a novel pathway explaining the estrogenic activity of PCBs. *Endocrinology* **141:**1897-1900.

Lans MC, Klasson-Wehler E, Willemsen M, Meussen E, Safe S and Brouwer A (1993) Structure-dependent, competitive interaction of hydroxy- polychlorobiphenyls, -dibenzo-p-dioxins and -dibenzofurans with human transthyretin. *Chem Biol Interact* **88:**7-21.

Lehmler HJ and Robertson LW (2001) Synthesis of hydroxylated PCB metabolites with the Suzuki-coupling. *Chemosphere* **45:**1119-1127.

Li H, Drouillard KG, Bennett E, Haffner GD and Letcher RJ (2003) Plasma-associated halogenated phenolic contaminants in benthic and pelagic fish species from the Detroit River. *Environ Sci Technol* **37:**832-839.

Locuson CW and Tracy TS (2007) Comparative modelling of the human UDP-glucuronosyltransferases: insights into structure and mechanism. *Xenobiotica* **37:**155-168.

Machala M, Blaha L, Lehmler HJ, Pliskova M, Majkova Z, Kapplova P, Sovadinova I, Vondracek J, Malmberg T and Robertson LW (2004) Toxicity of hydroxylated and quinoid PCB metabolites: inhibition of gap junctional intercellular communication and activation of aryl hydrocarbon and estrogen receptors in hepatic and mammary cells. *Chem Res Toxicol* **17:**340-347.

Maervoet J, Covaci A, Schepens P, Sandau CD and Letcher RJ (2004) A reassessment of the nomenclature of polychlorinated biphenyl (PCB) metabolites. *Environ Health Perspect* **112:**291-294.

Meerts IA, Lilienthal H, Hoving S, van den Berg JH, Weijers BM, Bergman Å, Koeman JH and Brouwer A (2004) Developmental exposure to 4-hydroxy-2,3,3',4',5-pentachlorobiphenyl (4-OH-CB107): long-term effects on brain development, behavior, and brain stem auditory evoked potentials in rats. *Toxicol Sci* **82:**207-218.

Radominska-Pandya A, Ouzzine M, Fournel-Gigleux S and Magdalou J (2005) Structure of UDP-glucuronosyltransferases in membranes. *Methods Enzymol* **400:**116-147.

Sacco JC (2006) Phase II biotransformation of xenobiotics in polar bear (Ursus maritimus) and channel catfish (Ictalurus punctatus) University of Florida

Sacco JC and James MO (2005) Sulfonation of environmental chemicals and their metabolites in the polar bear (Ursus maritimus). *Drug Metab Dispos* **33:**1341-1348.

Sandau CD, Ayotte P, Dewailly E, Duffe J and Norstrom RJ (2002) Pentachlorophenol and hydroxylated polychlorinated biphenyl metabolites in umbilical cord plasma of neonates from coastal populations in Quebec. *Environ Health Perspect* **110:**411-417.

Singh J, Dubey RK and Atal CK (1986) Piperine-mediated inhibition of glucuronidation activity in isolated epithelial cells of the guinea-pig small intestine: evidence that piperine lowers the endogeneous UDP-glucuronic acid content. *J Pharmacol Exp Ther* **236:**488-493.

Sinjari T and Darnerud PO (1998) Hydroxylated polychlorinated biphenyls: placental transfer and effects on thyroxine in the foetal mouse. *Xenobiotica* **28:**21-30.

Sjödin A, Hagmar L, Klasson-Wehler E, Björk J and Bergman Å (2000) Influence of the consumption of fatty Baltic Sea fish on plasma levels of halogenated environmental contaminants in Latvian and Swedish men. *Environ Health Perspect* **108:**1035-1041.

Tampal N, Lehmler HJ, Espandiari P, Malmberg T and Robertson LW (2002) Glucuronidation of hydroxylated polychlorinated biphenyls (PCBs). *Chem Res Toxicol* **15:**1259-1266.

Wang LQ, Falany CN and James MO (2004) Triclosan as a substrate and inhibitor of 3'-phosphoadenosine 5'-phosphosulfate-sulfotransferase and UDP-glucuronosyl transferase in human liver fractions. *Drug Metab Dispos* **32:**1162-1169.

Wang LQ, Lehmler HJ, Robertson LW, Falany CN and James MO (2005) In vitro inhibition of human hepatic and cDNA-expressed sulfotransferase activity with 3-hydroxybenzo[a]pyrene by polychlorobiphenylols. *Environ Health Perspect* **113:**680-687.

Wang LQ, Lehmler HJ, Robertson LW and James MO (2006) Polychlorobiphenylols are selective inhibitors of human phenol sulfotransferase 1A1 with 4-nitrophenol as a substrate. *Chem Biol Interact* **159:**235-246.

Yamamura N, Imura-Miyoshi K and Naganuma H (2000) Panipenum, a carbapenem antibiotic, increases the level of hepatic UDP-glucuronic acid in rats. *Drug Metab Dispos* **28:**1484-1486.

Zhivkov V, Tosheva R and Zhivkova Y (1975) Concentration of uridine diphosphate sugars in various tissues of vertebrates. *Comp Biochem Physiol B* **51:**421-424.

Footnotes

This research was supported in part by US Public Health Service Grants P42 ES07375 and P42 ES013661.

Figure Legends

Figure 1. Structures of polychlorinated biphenylols used as substrates for glucuronidation in microsomes from channel catfish liver and proximal intestine.

Figure 2. Validation of the extraction method for assay of OH-PCB glucuronidation. The figure shows TLC radiochromatograms of the ethyl acetate extract and aqueous phase from incubation of hepatic microsomes with ^{14}C-UDPGA and 4′-OH-CB121 or no substrate, as described in the methods section. Arrows indicate the origin, front and bands corresponding to the glucuronide conjugate, glucuronic acid and UDPGA. The ethyl acetate extracts were evaporated to dryness under nitrogen and the residues reconstituted in ethanol or Tris buffer. Lane 1, ethyl acetate extract of an incubation with 4′-OH-CB121, showing the glucuronide conjugate; lane 2, ethyl acetate extract from an incubation with no substrate; lane 3, β-glucuronidase-treated ethyl acetate extract from an incubation with 4′-OH-CB121, showing hydrolysis of the glucuronide conjugate to ^{14}C-glucuronic acid; lane 4, ethyl acetate extract from an incubation with 4′-OH-CB121, subsequently incubated with buffer, showing stability of the conjugate; lane 5, aqueous phase from an incubation with 4′-OH-CB121, showing UDPGA but no glucuronide conjugate; lane 6, aqueous phase from an incubation with no substrate.

Figure 3. Representative kinetic plots of the glucuronidation of OH-PCBs in 4 individual channel catfish. (A) Michaelis-Menten plot for 4′-OH-CB159 by hepatic microsomes. (B) Hill plot for 4′-OH-CB112 by proximal intestinal microsomes.

Figure 4. Relationship between maximal rate of glucuronidation of OH-PCBs in microsomes from channel catfish liver and proximal intestine. Each point represents the mean V_{max} for four fish.

Figure 5. Decrease in V_{max} values with the addition of a second chlorine atom flanking the phenolic group, while keeping the chlorine substitution pattern on the aphenolic ring constant, in the proximal intestine (A), and liver (B).

Figure 6. Relationship of V_{max} to pKa of the phenolic hydroxyl group in liver (A) and proximal intestine (B). In each graph, the line indicates the trend for V_{max} to be higher for OH-PCBs with neutral pKa values compared to those with lower or higher values.

Figure 7. Concentrations of UDPGA in liver and whole intestinal mucosa of the channel catfish. Each point represents the mean of duplicate determinations for samples of individual liver and whole intestinal mucosa.

DMD Fast Forward. Published on January 7, 2008 as DOI: 10.1124/dmd.107.019596
This article has not been copyedited and formatted. The final version may differ from this version.

Table 1. Kinetic parameters (Mean ± SD; *n*=4) for the co-substrate UDPGA in the glucuronidation of three OH-PCBs.

	OH-PCB concentration (μM)	V_{max} (app) (nmol/min/mg)	K_m (app) (μM)
Liver			
4′-OHCB-35	500	0.87 ± 0.20	697 ± 246
4′-OHCB-72	500	0.60 ± 0.10	684 ± 323
Intestine			
4′-OHCB-69	200	0.20 ± 0.11	27 ± 14

DMD Fast Forward. Published on January 7, 2008 as DOI: 10.1124/dmd.107.019596
This article has not been copyedited and formatted. The final version may differ from this version.

Table 2. Kinetic parameters (Mean ± SD; *n*=4) for the glucuronidation of 4-OH-BP and OH-PCBs. Units for K_m, V_{max} and enzyme efficiency are μM, pmol/min/mg, and μL/min/mg protein, respectively.

Substrate	Intestine			Liver		
	V_{max} (app)	K_m (app)	Efficiency	V_{max} (app)	K_m (app)	Efficiency
4-OH-BP	43 ± 10	599 ± 110	0.07 ± 0.02	182 ± 78	502 ± 235	0.48 ± 0.36
4-OH-CB1	504 ± 126	157 ± 18	3.2 ± 0.6	812 ± 326	150 ± 60[a]	5.5 ± 0.6
4-OH-CB2	417 ± 57	572 ± 47	0.73 ± 0.11	2,277 ± 849	583 ± 95	3.95 ± 1.34
4′-OH-CB3	399 ± 110	412 ± 54	1.0 ± 0.4	317 ± 90	237 ± 58	1.4 ± 0.5
4′-OH-CB9	410 ± 99	297 ± 55	1.4 ± 0.3	751 ± 390	626 ± 318	1.4 ± 0.8
4-OH-CB14	255 ± 59	387 ± 65	0.67 ± 0.19	2,022 ± 936	614 ± 202	3.31 ± 0.86
4′-OH-CB18	693 ± 223	15 ± 1[a]	47 ± 18	1,225 ± 699	57 ± 24	20.8 ± 4.0
4′-OH-CB35	784 ± 348	265 ± 85	2.91 ± 0.87	2,838 ± 1456	455 ± 89[a]	6.67 ± 3.55
4-OH-CB39	220 ± 90	134 ± 36	1.61 ± 0.37	1,716 ± 536	242 ± 76	7.42 ± 2.28
4′-OH-CB68	213 ± 91	119 ± 75	2.09 ± 0.93	ND[b]	ND	ND
4′-OH-CB69	751 ± 253	42 ± 21	20.7 ± 7.2	2,774 ± 1153	1,071 ± 410	2.81 ± 1.18
4′-OH-CB72	401 ± 236	183 ± 126	2.43 ± 0.33	ND	ND	ND
4′-OH-CB79	124 ± 36	87 ± 21	1.47 ± 0.46	869 ± 318	476 ± 201	1.91 ± 0.50
4′-OH-CB106	431 ± 60	183 ± 58	2.52 ± 0.75	1,579 ± 645	798 ± 122	2.00 ± 0.79
4′-OH-CB112	401 ± 67	163 ± 24[a]	2.52 ± 0.62	2,144 ± 1007	1,643 ± 545	1.40 ± 0.63
4′-OH-CB121	220 ± 39	130 ± 21	1.70 ± 0.24	1,046 ± 408	207 ± 97	5.27 ± 1.32
4′-OH-CB159	188 ± 66	213 ± 136	1.07 ± 0.46	681 ± 141	318 ± 91	2.26 ± 0.63
4′-OH-CB165	163 ± 26	137 ± 44	1.25 ± 0.30	404 ± 116	111 ± 28	3.77 ± 1.07

[a] S_{50} value given in place of K_m due to atypical kinetics

[b] Not done

DMD Fast Forward. Published on January 7, 2008 as DOI: 10.1124/dmd.107.019596
This article has not been copyedited and formatted. The final version may differ from this version.

Table 3. Comparison of composite kinetic parameters for the glucuronidation of OH- PCBs grouped according to the number of chlorine atoms flanking the phenolic group.

Organ	Parameter	Flanking chlorines		
		0	1	2
Liver	V_{max} (app), pmol/min/mg	776 ± 128[a,b]	2247 ± 226[c]	1123 ± 148[a,b]
	K_m (app), μM	267 ± 67[e]	856 ± 110[f]	323 ± 43[e]
Intestine	V_{max} (app), pmol/min/mg	501 ± 46[b]	556 ± 56[b]	223 ± 21[d]
	K_m (app), μM	221 ± 40[e,g]	245 ± 42[e,g]	162 ± 20[g]

Results shown are mean ± S.E. In liver, n=16 for 0 flanking Cl atoms, n=20 for 1 flanking Cl atoms and n=24 for 2 flanking Cl atoms. In intestine, n=16 for 0 flanking Cl atoms, n=20 for 1 flanking Cl atoms and n=32 for 2 flanking Cl atoms.

For any one parameter, values with the same superscript letter are not significantly different from one another. Those with different superscript letters are significantly different, $p<0.01$

Figure 1

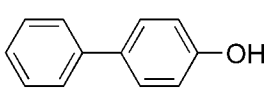

4-OH-BP

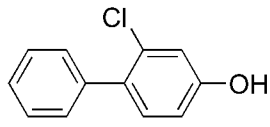

4-OH-CB1

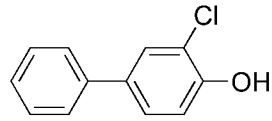

4-OH-CB2

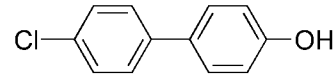

4'-OH-CB3

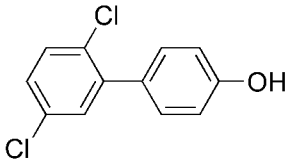

4'-OH-CB9

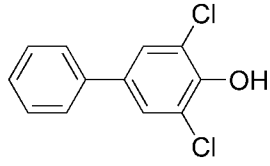

4-OH-CB14

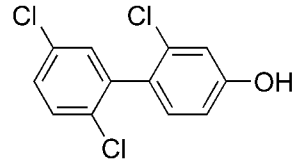

4'-OH-CB18

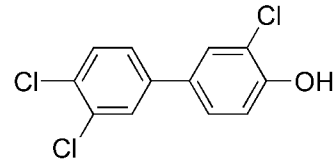

4-'OH-CB35

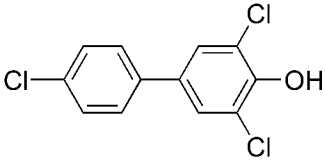

4-OH-CB39

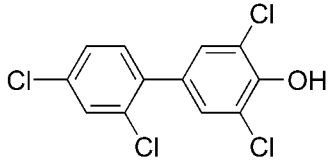

4'-OH-CB68

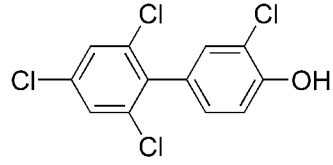

4'-OH-CB69

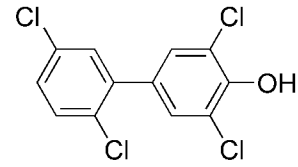

4'-OH-CB72

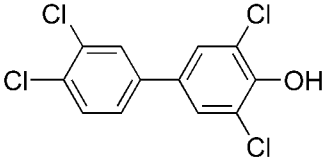

4'-OH-CB79

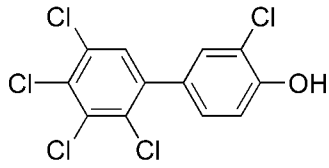

4'-OH-CB106

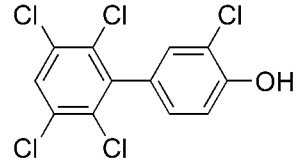

4'-OH-CB112

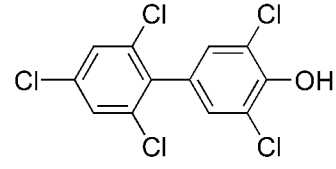

4'-OH-CB121

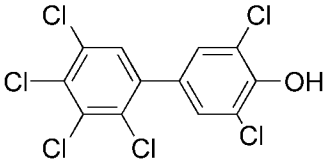

4'-OH-CB159

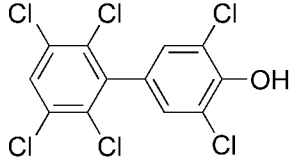

4'-OH-CB165

Figure 2

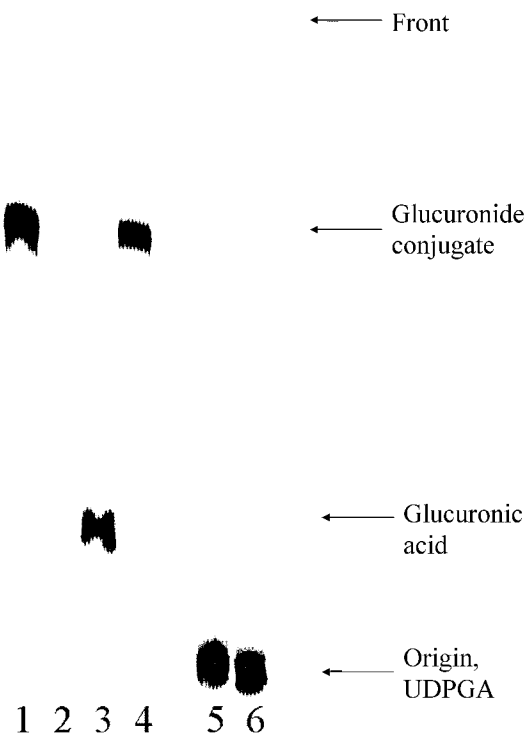
Front
Glucuronide conjugate
Glucuronic acid
Origin, UDPGA
1 2 3 4 5 6

Figure 3

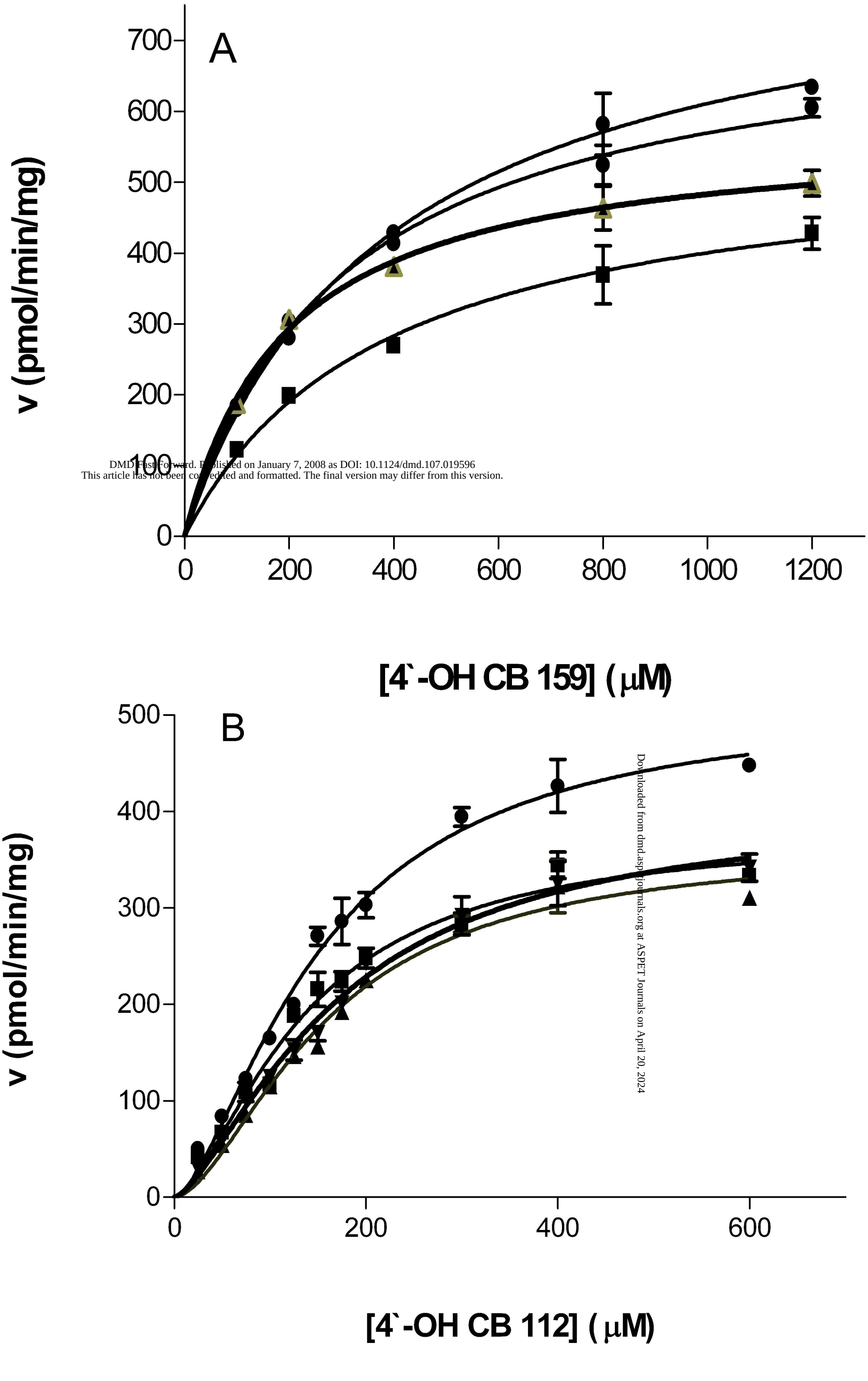

DMD Fast Forward. Published on January 7, 2008 as DOI: 10.1124/dmd.107.019596
This article has not been copyedited and formatted. The final version may differ from this version.

Figure 4

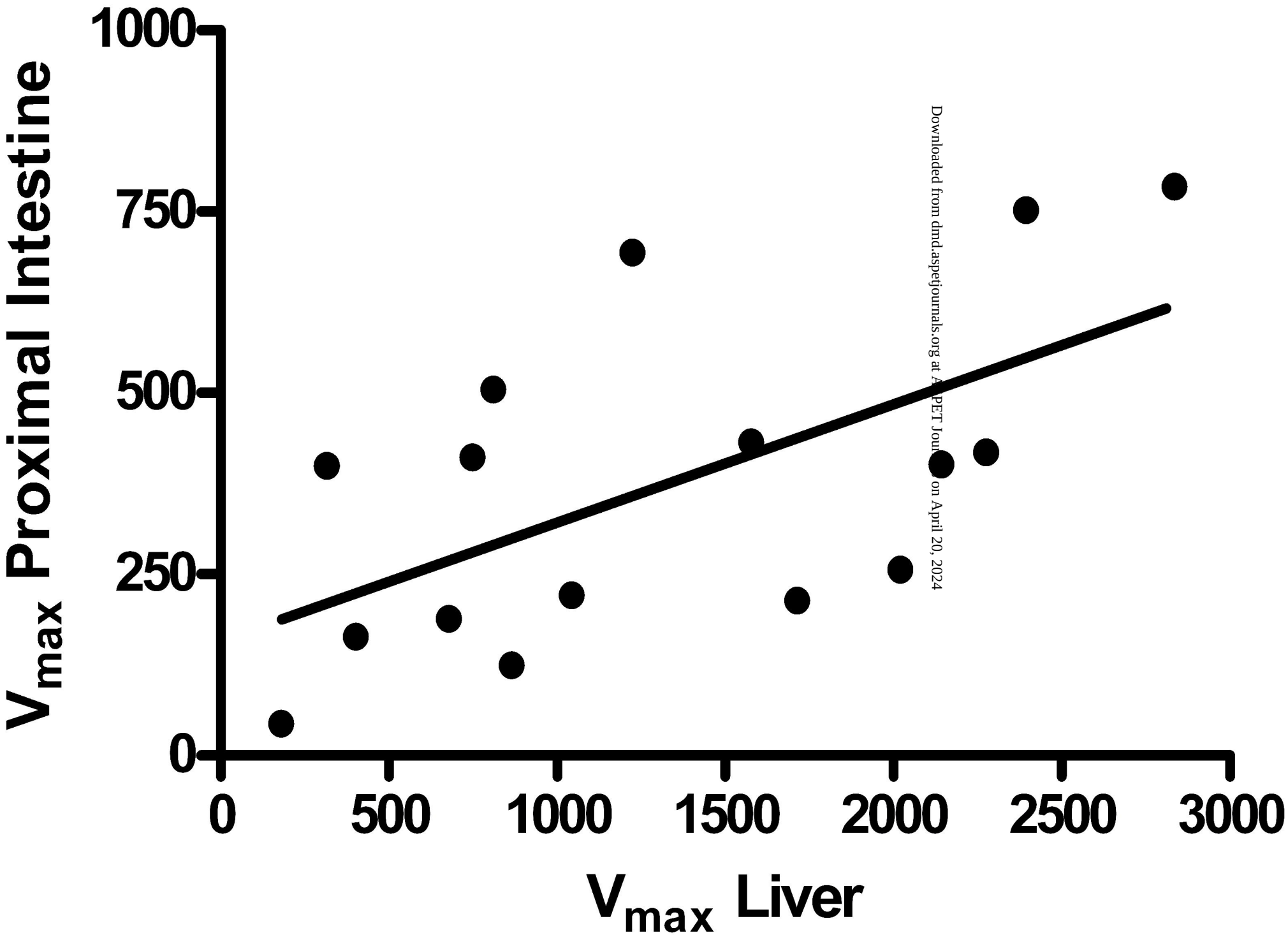

Figure 5

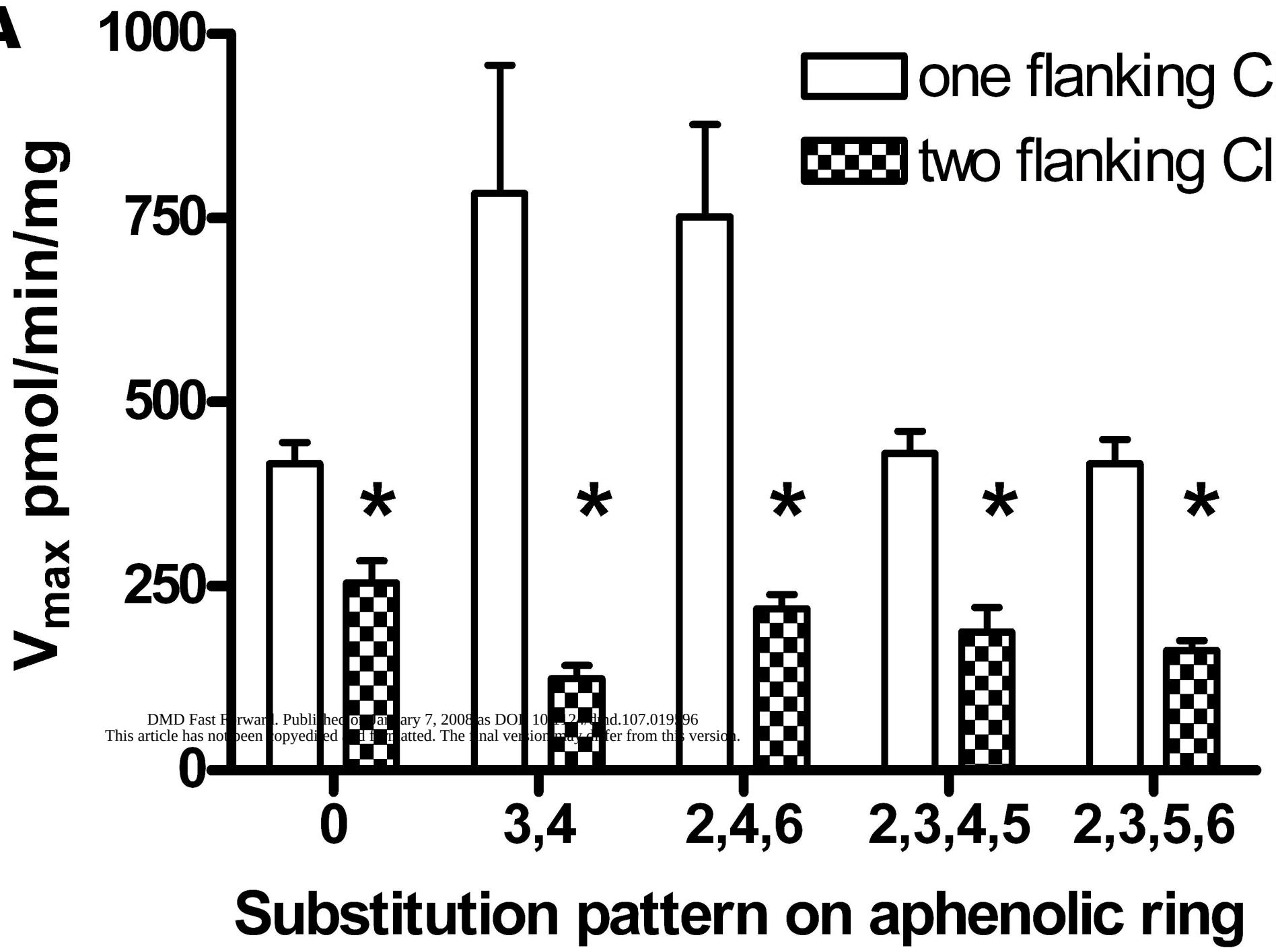

Figure 6

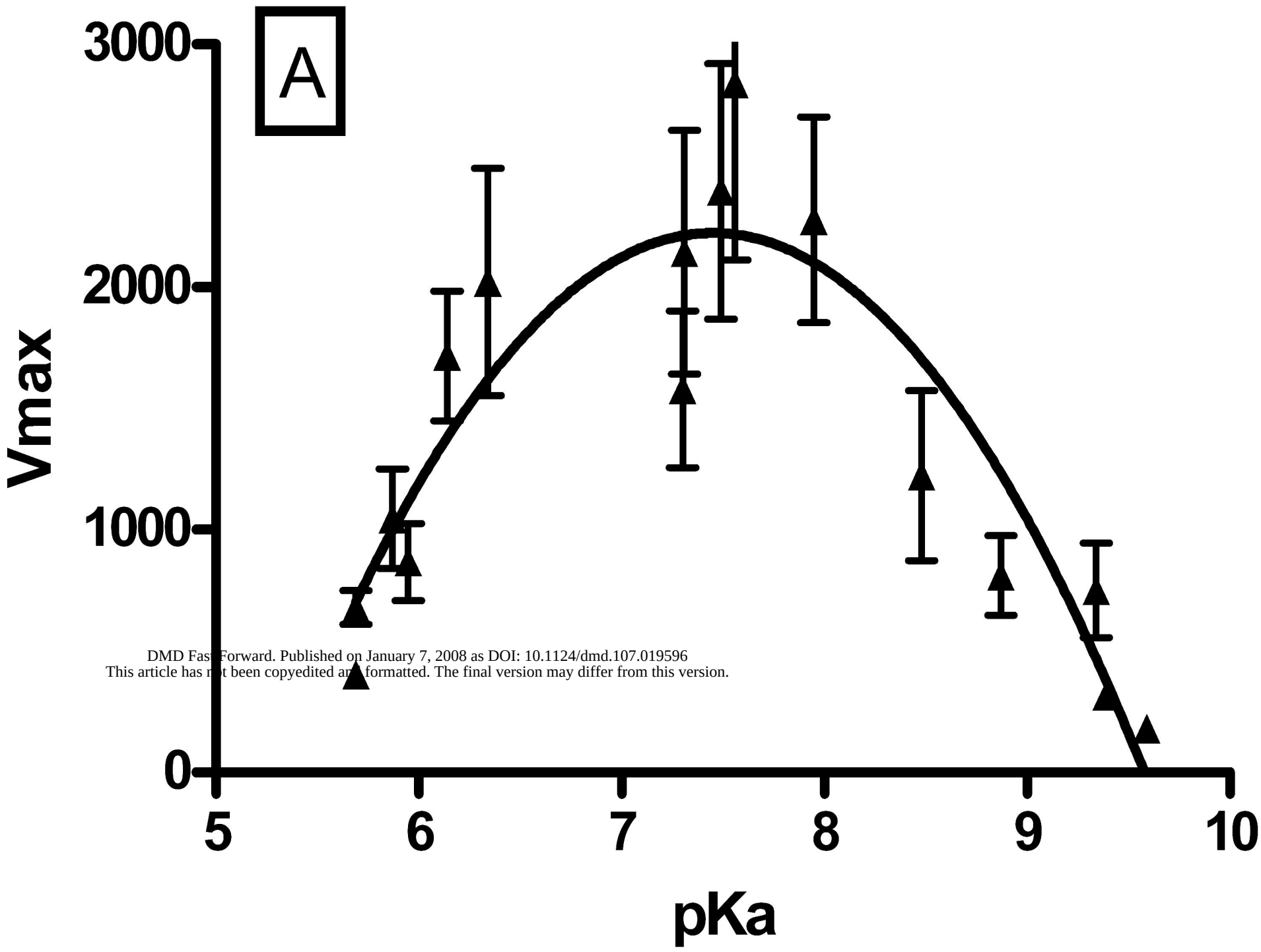

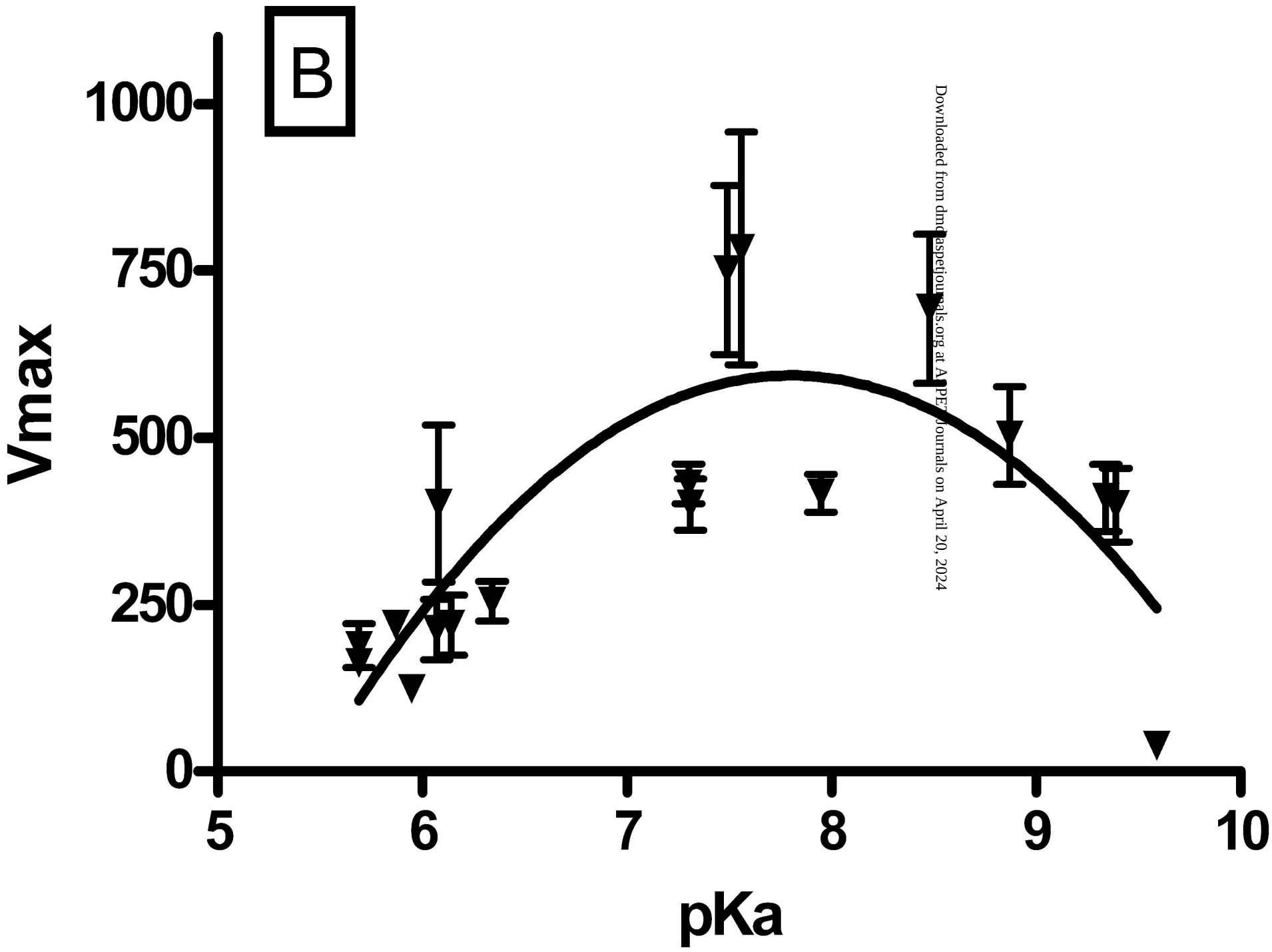

Figure 7